Soil Biology and Biochemistry 168 (2022) 108634

Contents lists available at ScienceDirect

Soil Biology and Biochemistry

journal homepage: www.elsevier.com/locate/soilbio

Stable isotopes reveal that fungal residues contribute more to mineral-associated organic matter pools than plant residues

Saskia Klink [a], Adrienne B. Keller [b,1], Andreas J. Wild [a,e], Vera L. Baumert [d,e], Matthias Gube [f], Eva Lehndorff [c], Nele Meyer [c], Carsten W. Mueller [g], Richard P. Phillips [b], Johanna Pausch [a,*]

[a] Department of Agroecology, Bayreuth Center of Ecology and Environmental Research (BayCEER), University of Bayreuth, 95440 Bayreuth, Germany
[b] Department of Biology, Indiana University, Bloomington, IN, 47405, USA
[c] Soil Ecology, Bayreuth Center of Ecology and Environmental Research (BayCEER), University of Bayreuth, 95448, Bayreuth, Germany
[d] Bavarian State Research Center for Agriculture, Institute for Organic Farming, Soil and Resource Management, 85354, Freising, Germany
[e] Chair of Soil Science, School of Life Sciences, Technical University of Munich, 85354, Freising, Germany
[f] Soil Science of Temperate Ecosystems, Büsgen-Institute, Georg-August University Göttingen, 37077, Göttingen, Germany
[g] Department of Geosciences and Natural Resource Management, University of Copenhagen, 1350, Copenhagen K, Denmark

ARTICLE INFO

Keywords:
Amino sugars
Mineral-associated organic matter
MEMS hypothesis
Particulate organic matter
Stable isotopes
Soil organic matter dynamics

ABSTRACT

We still lack crucial knowledge about the contribution of plant *vs*. microbial residues to specific SOM pools, particularly the relative contribution of arbuscular (AM), ectomycorrhizal (ECM), and saprotrophic (SAP) fungi.

We investigated sources of particulate and mineral-associated organic matter (POM and MAOM) around trees with distinct mycorrhizal types, *Liriodendron tulipifera* (AM-association) and *Quercus alba* (ECM-association), in a temperate deciduous forest in Indiana, USA. Combining ^{13}C and ^{15}N natural abundance analyses with measurements of microbial residues using amino sugars, the isotope signatures of large, medium and small-sized POM and MAOM fractions were compared with those of leaves, roots and biomass of mycorrhizal and saprotrophic fungi. A Bayesian inference isotope mixing model calculated sources of C and N to SOM fractions.

While the isotope composition of POM resembled that of plants, MAOM was close to fungal values. This was confirmed by mixing model calculations and microbial residue analysis, which additionally and independent from tree partner suggested saprobic fungi contributing with 4–53% to POM and 23–42% to MAOM, as opposed to ECM contributions.

Our results suggest fungal, not plant residues, as the source of the most putatively stable OM pool; thus, altering fungal communities may enhance efforts to increase long-term soil C storage.

1. Introduction

Soil organic matter consists of a multitude of organic compounds forming a continuum of decay, ranging from fresh detritus to highly processed organic matter either in the form of particles or associated with mineral surfaces (Schmidt et al., 2011; Lehmann and Kleber, 2015). Along the path of SOM formation and turnover, entities of different size, complexity and degree of decomposition are established (Angst et al., 2021; Lehmann et al., 2020). Hence, distinct fractions of organic matter can be defined in soil, which differ in their formation, chemical composition, persistence, and function (Golchin et al., 1994; Lavallee et al., 2020). Nevertheless, we lack a foundational understanding of the source and stability of most SOM fractions.

Due to the complex continuum of SOM compartments differing in composition and turnover time, characterizing and understanding SOM dynamics requires separation of SOM into measurable fractions in order to elucidate the fate of certain carbon (C) pools (Poeplau et al., 2018). One approach to elucidate differences between C and nitrogen (N) storage and sequestration in organic matter (OM) particles *vs*. OM associated with mineral surfaces and thus predict SOM dynamics, is the separation into particulate organic matter (POM) and mineral-associated organic matter (MAOM) fractions (Golchin et al., 1994; Lavallee et al., 2020; Angst et al., 2021). Particulate OM is dominated by structural C compounds of plant origin (Baldock and

* Corresponding author: Department of Agroecology, GEO I, Bayreuth Center of Ecology and Environmental Research (BayCEER), University of Bayreuth, 95440, Bayreuth, Germany
E-mail address: johanna.pausch@uni-bayreuth.de (J. Pausch).
[1] Current address Adrienne Keller: Department of Ecology, Evolution, and Behavior, University of Minnesota, Saint Paul, 55108, USA

https://doi.org/10.1016/j.soilbio.2022.108634
Received 10 November 2021; Received in revised form 14 March 2022; Accepted 16 March 2022
Available online 26 March 2022

Skjemstad, 2000; Lavallee et al., 2020; Angst et al., 2021) and the major part of the C-rich, complex inputs to POM are relatively vulnerable to microbial decay (Christensen, 2001; Lützow et al., 2007; Cotrufo et al., 2019). In contrast, part of the POM pool can be highly persistent due to occlusion within aggregates and high aromaticity or aliphaticity (Mueller and Koegel-Knabner, 2009). In contrast to POM, which is derived principally from plant inputs, MAOM consists mainly of microbial residues (Kopittke et al., 2018, 2020), although plant biomolecules, e.g., leachates from litter, may contribute (Mikutta et al., 2019; Sokol and Bradford, 2019; Angst et al., 2021).

It has been proposed that the contribution of microbial residues to MAOM is higher in systems with high litter quality (meaning a lower C:N ratio and more easily decomposable litter) and environmental conditions optimal for microbial activity and growth (e.g., favorable soil pH and moisture; cf. Microbial Efficiency-Matrix Stabilization (MEMS) framework (Cotrufo et al., 2013)). While numerous studies confirmed the MEMS framework (e.g. Bradford et al., 2013; Craig et al., 2018; Cyle et al., 2016; Rumpel et al., 2015), finding greater MAOM-N in AM-dominated plots with faster decaying litter than in ECM plots (Craig et al., 2018) or highlighting the importance of the microbial use efficiency (Rumpel et al., 2015), other studies challenged the MEMS framework. Castellano et al. (2015) highlighted the consideration of C saturation of the mineral surface and of litter quantity for MAOM formation. Further, as discussed in Evans et al. (2020), priming of microorganisms by high quality litters appears to increase MAOM mineralization (see also Córdova et al., 2018). Finally, Huang et al. (2019) underpinned the importance of lignin-derived C contributing to MAOM in addition to microbial residues. Thus, further research appears necessary to decipher the processes of MAOM formation and the role of microbial inputs in dependence of litter quality.

Among soil microorganisms, root-associated mycorrhizal fungi make up more than 30% of microbial biomass (Högberg and Högberg, 2002; Frey, 2019). Mycorrhizal fungi use plant-derived C for biomass production and metabolism (e.g. respiration), releasing C to soil from living hyphae (e.g., organic acids and extracellular enzymes) and dead hyphal biomass (Frey, 2019). In this way, mycorrhizal hyphae can contribute directly to the POM and MAOM fractions (Frey, 2019; Godbold et al., 2006). Further, free-living saprotrophs also produce their own residues and exudates (e.g. Verbruggen et al., 2017), and form necromass upon death that may be attached to mineral surfaces (Li et al., 2015; Joergensen, 2018; Witzgall et al., 2021). Recently it was shown that via the expansion of their mycelium, fungi can translocate C into deeper soil layers where fungal exudates and residues can bind to minerals (Witzgall et al., 2021). While many factors are known to influence microbially-mediated SOM dynamics (Fan and Liang, 2015; Liang et al., 2019), we still know remarkably little about the contribution from varying microbial sources such as mycorrhizal or saprotrophic (SAP) fungi affecting the various SOM fractions' capability of C and N storage.

Tracking the input from different origins to SOM fractions is methodologically challenging owing to the intimacy of the associations between roots and microbes and the dynamic nature of root-microbial and microbe-microbe interactions. Stable isotope natural abundance approaches are a valuable tool to trace the transfer of plant and fungal C and N inputs to SOM fractions, as stable isotopes possess both information about the ongoing process (process information) and the origin of the signature (source information) (Fry, 2008). For example, plants are relatively depleted in ^{13}C compared to most soil fungi (e.g. Högberg et al., 1999) owing to the fractionation that occurs in heterotrophs from enzymatic decomposition of cellulose in wood or litter (Gleixner et al., 1993; Kohzu et al., 1999). The ^{15}N of fungi depends, in large part, on the source of N (Gebauer and Taylor, 1999), and whether N is shared with an associated plant or not (cf. Gebauer and Dietrich, 1993). Thus, along the process of leaf litter decay to form POM and MAOM, a shift from relatively depleted plant-related C and N isotopic ratios to relatively enriched fungal-related C and N isotopic ratios should occur. Although most of the C that mycorrhizal fungi receive is plant-derived, mycorrhizal fungi $\delta^{13}C$ isotopic signatures often are more enriched relative to those of the plant. While previous investigations have uncovered variations in the isotopes of plant and microbial inputs, we still lack understanding of the linkages of these inputs to fast and slow-cycling SOM fractions in forests.

We sought to investigate the sources of POM and MAOM in a temperate deciduous forest in Indiana, USA around two dominant tree species - tulip poplar (*Liriodendron tulipifera* L.) and white oak (*Quercus alba* L.). These species differ in multiple traits and characteristics, such as the type of mycorrhizal fungi they associate with (arbuscular mycorrhizal fungi for tulip poplar; ectomycorrhizal fungi for white oak), their litter quality (tulip > oak; Midgley et al., 2015), and the soil microbial communities they promote (Rosling et al., 2016; Mushinski et al., 2020). Due to ECM fungi generating a less favorable environment for SAP fungi and competition between ECM and SAP fungi (cf. Gadgil effect, e.g. Fernandez and Kennedy, 2016), in ECM-associated systems we expect ECM fungi as main contributors to SOM. Conversely in AM-associated systems AM or SAP fungi should be the primary contributors. Interactions between AM and SAP fungi may support nutrient acquisition in the AM-system (Verbruggen et al., 2017; Cheeke et al., 2021). We tracked the transfer of plant and fungal inputs into various SOM pools by comparing the isotopic signatures of different fungal groups to isotopic signatures of multiple POM and MAOM fractions. A Bayesian Inference isotopic mixing model was applied in order to get an idea about the relative contribution of plant- and fungal-derived inputs to the POM and MAOM fractions. Moreover, we used analyses of amino sugars (cell wall components of bacteria and fungi) as an independent parameter from that of isotopes to classify which microbial groups contribute to soil C storage in different SOM fractions (Amelung, 2001). Estimates of the contribution of fungal and bacterial compounds to soil C will aid to describe how microbial products contribute to SOM formation. Combining stable isotope natural abundance analyses and amino sugar analyses, we tested the following predictions:

(i) Plant residues are the predominant source of POM-C and –N, while fungal residues are the dominant source of MAOM-C and –N. This will be represented by a gradual isotopic enrichment in ^{13}C and ^{15}N from POM to MAOM fractions.
(ii) Ectomycorrhizal (ECM) fungi will be the dominant source of C and N to SOM fractions under white oak (ECM-associating trees) while saprotrophic (SAP) fungi contributions will be dominant under tulip poplar (AM-associating trees).
(iii) Amino sugar analyses will show bacteria affecting soil C storage for both POM and MAOM fractions and a shift to higher fungal contribution for MAOM fractions.

2. Materials and methods

2.1. Study site

The study site Moore's Creek is a *c*. 80-year-old temperate deciduous forest in south-central Indiana, USA, which is part of Indiana University's Research and Teaching Preserve (39°05' N, 86°28' W, *cf*. Midgley and Phillips, 2016). The region is characterized by a humid continental climate with a mean annual precipitation of *c*. 1200 mm and a mean annual temperature of 11.6 °C. Moore's Creek was unaffected during the southern advance of the last glacial event (the Wisconsin glaciation) and as such, there is steep ridge-ravine topography, and nutrient-poor silty-loam soils derived from sandstone and shale (mesic Typic Dystrochrepts) with soil pH < 5.23 (Phillips et al., 2013). More detailed information about the study site is given in Phillips et al. (2013), Midgley and Phillips (2019) and Mushinski et al. (2019). Dominant tree species at the site include trees that associate with arbuscular mycorrhizal fungi (*Liriodendron tulipifera* L., *Acer saccharum* Marshall, *Sassafras albidum* (Nutt.) and *Prunus serotina* Ehrh.) and those associating with ectomycorrhizal (ECM) fungi (*Quercus alba* L., *Fagus*

grandifolia Ehrh., *Quercus rubra* L., *Quercus velutina* Lam. and *Carya glabra* Mill.). Sampling was conducted in June (peak growing season) and October (late growing season) 2018 around five canopy trees: two individuals of *Q. alba* L. (white oak) and three individuals of *L. tulipifera* L. (tulip poplar). Additionally, two individuals of *F. grandifolia* Ehrh. (American beech) and *A. saccharum* Marshall (sugar maple) were sampled only for stable isotope analysis (Supporting material Fig. S1). To control for topography, only trees growing on the upper third of north-facing ridges were chosen. The distance between each focal tree to a neighboring canopy tree was at least 3 m.

2.2. Sampling procedure

Mature, healthy, sunlit leaves (6–7 per tree species) of each focal tree were collected by shooting twigs (shotgun) or by cutting leaves from freshly broken twigs. Roots (first four root orders) were excavated approximately 0.5 m from each tree trunk at four spots and traced back to the target tree species to ensure correct tree association. In the lab, roots were washed with water, cleaned from debris with tweezers and sub-divided for stable isotope analysis (4 composite samples per tree species), fungal isolation, and DNA analyses. Arbuscular mycorrhizal (AM) fungi were isolated from roots of AM-associated tulip poplar via a mechanical isolation approach presented in Klink et al. (2020) and pooled to six composite samples to increase sample mass for isotopic analyses. This procedure was chosen over soil isolation to reduce the impact of other soil fungi on isotopic patterns and to increase the abundance of AM fungi. However, the presence of other fungal root endophytes, such as dark septate endophyte (DSE) fungi could not be excluded completely. For ECM-associated white oak roots, root tips with ectomycorrhizal (ECM) fungal sheath were separated and pooled into three composite samples to increase sample amount for isotopic measurements. Under each tulip poplar tree, sporocarps of 6 ECM and 12 SAP fungi (6 on wood, 6 on soil) were collected, and under each white oak tree 6 ECM and 4 SAP fungi (3 on wood, 1 on soil) were collected. The selection of both soil and wood SAPs was done in order to trace the effect of different food sources on SAP fungal isotopic signature for the specific habitat. All samples were collected within a radius of 2 m of each tree trunk and photo-documented. Wood and leaf litter, which are substrates for growing fungi, were collected. Recently fallen leaf litter was sampled from the soil surface in a 2 m radius around the tree trunk. Bulk soil was collected with a PVC soil corer (5 cm diameter) to a depth of 15 cm at four locations around each tree trunk. Bulk soil was sieved to 2 mm, cleaned of root particles and stones, weighed, and divided into one sub-sample for bulk analysis and one sub-sample for soil fractionation. For transportation and until further processing in the lab, leaf samples were stored in paper bags, and root, fungi, and soil samples were put in zip-lock bags on ice.

2.3. Soil fractionation

The bulk soils were subjected to a combined particle size and density fractionation in order to quantify the contribution of POM *vs*. MAOM to the overall C and N storage as well as the fractions' elemental and isotopic composition (cf. Mueller et al., 2014). Sub-samples (30 g) of bulk soil from white oak and tulip poplar soils were separated into multiple POM and MAOM fractions using a modified particle size and density fractionation method (Supporting material Fig. S2; Amelung and Zech (1999) and Mueller et al. (2014)). Bulk soil was suspended with deionized water (1:5, m:v) and capillary saturated for 1 h. Next, ultrasonic dispersion (SonoplusHD2200, Bandelin, Berlin, Germany) with an energy input of 440 J ml^{-1} (Amelung and Zech, 1999, probe tip at 15 mm) was applied to ensure strong dispersion of soil aggregates while organic matter structure was retained (Schmidt et al., 1999). Sonicated samples were subsequently separated by wet sieving using sieves of 63 μm and 20 μm mesh sizes. This resulted in size fractions of >63 μm, > 20 μm and <20 μm. To yield clean POM and MAOM fractions, these particle size fractions were further separated based on their density using sodium polyungstrate (SPT; 1.8 g cm^3). This allowed to recover POM floating on the SPT solution free from mineral particles, and MAOM sank down as heavy sediment free of POM. The resulting six fractions (>63 μm (MAOM), >20 μm (MAOM), <20 μm (MAOM), >63 μm (POM), >20 μm (POM), <20 μm (POM)) were cleaned from residues of SPT by rinsing them with deionized water and repeated centrifugation (>63 μm and >20 μm MAOM) or by pressure filtration (<20 μm fractions) with deionized water until an electric conductivity below 5 μS cm^{-1} was reached in the percolated water. Samples were subsequently freeze-dried, finely ground using a ball mill, and stored in desiccators until further processing. Due to the low C- and N-content of the fraction >20 μm (MAOM), no reliable stable isotope measurements could be conducted for this fraction. The average recovery of the soil fractionation process was 97.8% ± 0.5. In total, the soil fractionation resulted in $n = 12$ for tulip poplar and $n = 8$ for white oak for each of the five analyzed soil fractions. Hereafter, these fractions will be referred to as large MAOM or large POM (>63 μm), medium POM (>20 μm) and small MAOM or POM (<20 μm).

Particle size fractionation is ecologically relevant given that the larger sand-sized fractions typically consist mostly of carbohydrate-rich POM, whereas POM and increasing amounts of MAOM (the smaller the fraction the higher the amount of mineral-associated OM) in the smaller silt or clay-sized fractions are more dominated by aliphatic and/or aromatic compounds (Wagai et al., 2009; Angst et al., 2017). Additionally, the formation of organo-mineral associations, mostly in fine sized mineral fractions, supports the stabilization of otherwise bioavailable carbohydrates and microbial residues (Schöning et al., 2005; Kopittke et al., 2020).

2.4. Stable isotope analyses

Plant leaves, roots, and fungal sporocarps were washed with deionized water, and roots and sporocarps were further cleaned of debris using tweezers. All samples were dried to constant weight (60 °C) for 48 h. Afterwards, samples were ground to fine powder in a ball mill (MM2, RETSCH, Haan, Germany) and stored in desiccators filled with silica gel. Due to their small size, mycorrhizal root tips of white oak were weighed into tin capsules without being ground.

For stable isotope analyses, ground samples were weighed into tin or silver capsules (for AM hyphae). An elemental analyzer isotope ratio mass spectrometer (EA-IRMS; Elemental Analyzer 1108, CE Instruments, Milan, Italy; ConFlo III interface, Thermo Fisher Scientific, Bremen, Germany; IRMS Delta S, Finnigan MAT, Bremen, Germany) was used to determine the ratios of $^{13}C/^{12}C$, $^{15}N/^{14}N$ and the C- and N-content of the samples. For AM hyphae, a μEA-IRMS (μElemental Analyzer, Eurovector, Pavia, Italy; ConFlo IV interface, Thermo Fisher Scientific, Bremen, Germany; IRMS Delta 5 plus, Thermo Fisher Scientific, Bremen, Germany) specialized for small samples was used.

The stable isotope natural abundances are expressed as δ-values relative to international standards. Delta-values were calculated according to equation (1), whereby R describes the ratio of the heavy to the light isotope.

$$\delta^{13}C \text{ or } \delta\ ^{15}N = (R_{sample}/R_{standard} - 1) \text{ x } 1000\ (‰) \quad \text{(Equation 1)}$$

Vienna-Pee Dee Belemnite (V-PDB; $R_{standard} = 0.0111802$) was the standard material for C and air was the standard for N ($R_{standard} = 0.0036765$). Calculation of C- and N- concentrations was done by calibrating with acetanilide ($C_6H_5NH(COCH_3)$). The reproducibility of the $\delta^{13}C$ and $\delta^{15}N$ stable isotope analyses was always below ±0.2‰.

2.5. Fungal identification

Fungal sporocarps were identified via macroscopic and microscopic features. Photographs of the sampled sporocarps are available on

iNaturalist project 'Fungi Moores Creek 2018'. Genera of ECM fungi comprised *Russula*, *Boletus*, *Hygrophorus*, *Laccaria*, *Cortinarius*, *Lactarius*, *Cantharellus*, *Inocybe* and *Tricholoma,* SAP fungi belonged to the genera *Laetiporus*, *Hygrocybe*, *Agaricus*, *Marasmius*, *Gymnopus*, *Lycoperdon*, *Rhodocollybia*, *Mycena*, *Stereum*, *Grifola*, *Lenzites*, *Singerocybe*, *Rhizomarasmius*, *Ramaria*, *Fuscoporia*, *Gymnopilus*, *Macrolepiota*, *Merulius*, *Ischnoderma*, *Psathyrella*, *Bisporella* and *Hymenochaete*. These identifications are broadly in line with soil DNA sequencing results by Eagar et al. (2021), who found that ECM soils were dominated in decreasing order of relative abundance by the families Russulaceae > Tricholomataceae and Amanitaceae > Hydnangiaceae (*Laccaria* genus), Clavulinaceae and Cortinariaceae. AM soils were dominated by Russulaceae > Mortierellaceae > Hygrophoraceae. Thus, the collected sporocarps captures most of the dominant fungal taxa at the site (except for Amanitaceae, Clavulinaceae).

DNA sequencing and analyses were performed at Leiden University, Netherlands for fungi in roots of tulip poplar and white oak. Tulip poplar roots hosted Glomeraceae, e.g. the genera *Rhizophagus* and *Archaeospora*, but also DSE and ECM fungi. For description of DNA handling refer to Supporting material Methods S1.

2.6. Amino sugar analysis

Amino sugar analyses were conducted using sub-samples of small MAOM and large POM to evaluate portions of microbial and plant residues, respectively. Amino sugars are correlated to microbial residues (Parsons, 1981) and used to calculate the contribution of bacterial- and fungal-derived C. Analysis of individual amino sugars glucosamine (GlcN), galactosamine (GalN), mannosamine (ManN), and muramic acid (MurN) was conducted according to Zhang and Amelung (1996). Specifically, Glucosamine is often considered as an indicator of fungal residues, whereas muramic acid is considered as an indicator of bacterial residues (Joergensen, 2018).

In brief, an amount of soil corresponding to 0.3 mg N was extracted by hydrolysis in 6 M HCl for 8 h at 105 °C after adding myo-inositol as internal standard. The hydrolysate was filtered and dried. The residue was dissolved with water, neutralized by adjusting the pH to 6.7 (±0.1) using KOH, and centrifuged. The supernatant was freeze-dried, dissolved with methanol, centrifuged, dried, dissolved with H_2O, and freeze-dried. Derivatization of amino sugars to aldononitrile acetates was conducted according to Guerrant and Moss (1984). Afterwards, a second internal standard (β-endosulfan) was added and samples were dried and dissolved in ethyl acetate–hexane (1:1, v/v).

The amino sugar derivatives were analyzed on a gas chromatograph (GC 2000, Shimadzu, Japan) equipped with an OPTIMA® column (30 m × 0.32 mm ID with 0.25 μm film thickness, Macherey-Nagel, Germany) using a flame ionization detector according to Zhang and Amelung (1996). Amino sugars were quantified using myo-inositol as first internal standard (for recovery calculation) and β-endosulfan as second internal standard (for quantification). Amino sugar identification was done using external standards (GlcN, GluN, ManN, and MurN). Bacterial C was calculated by multiplying MurN by a conversion factor of 45 (Appuhn and Joergensen, 2006). Fungal C was calculated according to equation (2) and in line with Appuhn and Joergensen (2006) and Faust et al. (2017), where 179.17 is the molecular weight of GlcN, 253.23 is the molecular weight of MurN, and 9 is a conversion factor from fungal GlcN to fungal residue C.

$$\mu g\ \text{fungal C}\ g^{-1}\ \text{soil} = (((\mu g\ \text{GlcN}\ g^{-1}\ \text{soil} / 179.17) - (2 \times \mu g\ \text{MurN}\ g^{-1}\ \text{soil} / 253.23)) \times 179.17) \times 9 \quad \text{(Equation 2)}$$

2.7. Data analysis

Software R version 3.6.1 (2019) and SigmaPlot version 11.0 (2008) were used for statistical analyses and figures. Shapiro Wilk's test indicated that the majority of the data set was not normally distributed and therefore a conservative statistical analysis using non-parametric tests was chosen. Kruskal-Wallis rank sum tests (χ^2) were performed to compare plant tissues, soil compartments, and fungi in $\delta^{13}C$ and $\delta^{15}N$ stable isotope natural abundances for each of the two tree species. The same procedure was performed for C-, N-content and C:N ratio data. Pairwise *post hoc* tests where then performed for the afore mentioned groups using Dunn's method for unequal sample sizes and the Tukey method when equal sample sizes were given. The Holm-Bonferroni correction was applied to adjust *P* values. For comparisons between tulip poplar and white oak for each aforementioned group, Mann-Whitney *U* tests were applied. For amino sugar analyses parametric *t*-tests were performed to compare tree species differences in amino sugar content, fungal C and fungal to bacterial C ratio (F:B) of large POM and small MAOM fractions. Statistical significance between groups (pairwise comparison) was tested for groups with $n = 3$ or higher. A level of significance of $\alpha = 0.05$ was set.

A Bayesian Inference isotopic mixing model (R package 'SIAR', version 4.2; Parnell et al., 2010; Parnell and Jackson, 2013) was applied to partition plant and fungal inputs into POM and MAOM fractions. This concentration-dependent mixing model allows for probability estimates of input proportions, while accounting for variability and uncertainty in parameters (Parnell et al., 2010). In addition to greater statistical power, the Bayesian Inference isotopic mixing model allows the inclusion of discrimination factors, prior information, and many sources of variability (Parnell et al., 2010; Bond and Diamond, 2011). Detailed information on the algebra of the model is given in Parnell et al. (2010). The model was informed with C and N isotopic data and, in order to increase the power of the model, with C and N concentrations of the sources leaves and fungal groups (AM, ECM, SAP) and of the POM and MAOM fractions. The model was not informed with fractionation factors for our dataset, as the variety of fractionation processes present could not be deciphered or are unknown. We are aware that this affects the precision of the model (cf. Parnell et al., 2010) but chose to avoid the inclusion of a large error due to unknown or indeterminate fractionation factors. For both tulip poplar and white oak datasets, 500,000 iterations and a burnin with initial discard of 50,000 were used, resulting in a 30,000 posterior draw output. After verification of normal distribution of posterior draw output data, we applied the Student's *t*-test to test for significant differences between the single input sources to SOM fractions. We are aware that the proportional contributions of the fungal groups identified by the Bayesian inference mixing model underly certain restrictions. Other contributors to MAOM fractions such as bacteria or viruses) were neglected for this model due to challenges in gaining their stable isotope signatures under field conditions. Therefore, the relative proportions of these groups contributing to MAOM fractions need to be subtracted from the proportions found for leaves and fungi in our study.

2.8. Accession numbers

Raw sequences have been deposited in the European Nucleotide Archive under the accession number PRJNA678944.

3. Results

3.1. Contribution of individual SOM fractions to total soil organic C

From the soil subsample used for particle size density fractionation ~3.33% organic C was recovered for both tulip poplar and white oak soils (Table 1). Distribution of C and N in SOM fractions was similar between tulip poplar and white oak, except for a higher C content in the small MAOM of tulip poplar compared to the small MAOM fraction of white oak (Table 1).

Table 1
C and N distribution (%) of SOM fractions of tulip poplar and white oak in relation to the bulk soil. Significant differences of C and N contents and C:N ratios of POM and MAOM fractions within tree species are indicated with superscripted small letters. Significant differences between SOM fractions of tulip poplar and white oak are indicated by superscripted capital letters.

	tulip poplar (AM)									white oak (ECM)								
	C [% of bulk soil C]			N [% of bulk soil N]			C/N			C [% of bulk soil C]			N [% of bulk soil N]			C/N		
Small POM	8.0^{b}	±	5	5.1^{b}	±	4	24.5^{b}	±	4	$9.8^{a,b}$	±	13	$5.3^{b,c}$	±	2	29.5^{b}	±	10
Medium POM	9.4^{b}	±	10	5.7^{b}	±	6.7	25.2^{b}	±	4	$10.5^{a,b}$	±	6	$5.6^{b,c}$	±	3	$28.9^{b,a}$	±	9
Large POM	17.4^{b}	±	19	8.9^{b}	±	12	34.1^{b}	±	8	$17.4^{b,c}$	±	14	8.8^{c}	±	6	29.5^{b}	±	6
Small MAOM	61.0^{cA}	±	29	73.0^{cA}	±	30	12.0^{a}	±	3	36.3^{cB}	±	17	42.4^{cB}	±	12	12.4^{c}	±	3
Medium MAOM	NA			NA			NA			NA			NA			NA		
Large MAOM	0.4^{a}	±	0	0.5^{aC}	±	3	13.4^{a}	±	4	0.2^{a}	±	5	$0.2^{a,cD}$	±	0	$15.6^{a,c}$	±	2
Sum POM	~34.8%			~19.7%						~37.6%			~19.7%					
Sum MAOM	~61.4%			~73.5%						~36.5%			~42.6%					

MAOM, mineral associated organic matter; POM, particulate soil organic matter. NA, not available.

3.2. Stable isotope natural abundances

Plant tissues were significantly depleted relative to fungal biomass in their ^{13}C and ^{15}N isotopes, and patterns were similar for tulip poplar and white oak (Fig. 1). Overall, saprotrophic fungi were the most ^{13}C enriched and mycorrhizal fungi were the most ^{15}N enriched. Further, a progressive enrichment in ^{13}C and ^{15}N occurred from POM to MAOM fractions and with decreasing particle size (i.e., the most ^{13}C and ^{15}N enriched fractions were the small MAOM fractions).

Significant differences between plant material, mycorrhizal fungi, SAP fungi and bulk soil were reported for white oak plots for both ^{13}C ($\chi^2 = 24.56$, df = 3, $P = 0$) and ^{15}N ($\chi^2 = 22.21$, df = 3, $P = < 0.001$). The same holds true for tulip poplar plots ($\delta^{13}C$: $\chi^2 = 32.33$, df = 3, $P < 0.001$; $\delta^{15}N$: $\chi^2 = 30.80$, df = 3, $P = < 0.001$). White oak plant material was significantly ^{13}C depleted relative to SAP fungi ($Z = -4.156$, $P = 0.001$) and soil ($Z = -2.89$, $P = 0.007$), and more ^{13}C ($Z = 3.150$, $P = 0.004$) and ^{15}N ($Z = 4.314$, $P < 0.001$) depleted than mycorrhizal fungi. Isotopic signatures of leaf litter were −29.3‰ in $\delta^{13}C$ and −4.3‰ in $\delta^{15}N$ for tulip poplar and −29.1‰ in $\delta^{13}C$ and −4.8‰ in $\delta^{15}N$ for white oak. Tulip poplar plant material was significantly ^{13}C depleted relative to SAP fungi ($Z = -5.641$, $P < 0.001$) and more ^{15}N depleted than mycorrhizal fungi ($Z = 5.458$, $P < 0.001$). Mycorrhizal fungi at tulip poplar plots were more ^{13}C depleted ($Z = -3.402$, $P = 0.002$) and more ^{15}N enriched relative to SAP fungi ($Z = 3.511$, $P = 0.001$). For SOM fractions, POM was more ^{13}C and ^{15}N depleted than MAOM for both white oak ($\delta^{13}C$: $U(16, 24) = 384$, $P < 0.001$; $\delta^{15}N$: $U(16, 24) = 348$, $P < 0.001$) and tulip poplar plots ($\delta^{13}C$: $U(24, 36) = 822.5$, $P < 0.001$; $\delta^{15}N$: $U(24, 36) = 775.5$, $P < 0.001$).

When comparing tulip poplar and white oak no significant differences were reported for plant material, mycorrhizal fungi, SAP fungi or bulk soil for either $\delta^{13}C$ or $\delta^{15}N$. However, MAOM fractions of white oak plots were significantly more ^{13}C enriched than those of tulip poplar plots ($U(16, 24) = 296.5$, $P = 0.004$). Regarding C:N ratios, the leaf litter, wood, and roots had the highest values, while fungal biomass had the lowest values (Supporting material Tables S1 and S2). Notably, the C:N ratio of the MAOM fractions (mean white oak: 14.03, mean tulip poplar: 12.70) were similar to those of the mycorrhizal fungi (mean white oak: 10.57, mean tulip poplar: 10.98; Supporting material Table S1).

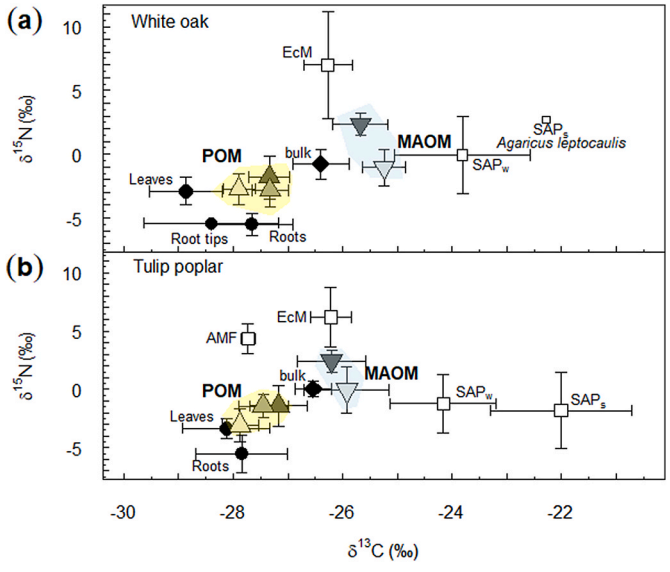

Fig. 1. Dual-isotope scatter plot of $\delta^{13}C$ and $\delta^{15}N$ mean values with standard deviation (SD) of (a) white oak and (b) tulip poplar. Circles represent plant tissues (leaf litter, roots, root tips or leaves), upwards triangles represent POM fractions (yellow background), downwards triangles MAOM fractions (blue background). Grey scales: light grey for large fractions (>63 μm particle size), medium grey for medium fractions (>20 μm particle size) and dark grey for small fractions (<20 μm particle size). Bulk soil is represented by a black diamond. Fungal biomass is indicated by white squares. AMF = arbuscular mycorrhizal fungi, ECM = ectomycorrhizal fungi, SAP_w = saprotrophic fungi on wood, SAP_s = saprotrophic fungi on soil. POM = particulate organic matter, MAOM = mineral-associated organic matter. (For interpretation of the references to colour in this figure legend, the reader is referred to the Web version of this article.)

3.3. Plant and fungal contributions to POM and MAOM fractions

Overall, our Bayesian Inference mixing model indicated that the POM fractions were dominated by plant inputs and the MAOM fractions were dominated by fungal inputs, with few differences between tulip *vs.* oak soils (Fig. 2, Supporting material Figs. S3 and S4). For both tulip poplar and white oak the mixing model calculated a predominantly plant-derived contribution to small, medium, and large POM (tulip poplar leaves: 7–50%, tulip poplar roots: 18–54%; white oak leaves: 24–52%, white oak roots: 29–62%). Free-living SAP fungal inputs contributed to POM with a probability of about 4–53%, while the probability of mycorrhizal fungi contribution was lower (ECM: 1–12%; AM: 1–4%). With decreasing particle size of POM, fungal contribution slightly increased to a maximum of 53% for SAP and 12% for ECM. For MAOM fractions, fungal inputs (2–63%) dominated over plant inputs (1–39%) for both tulip poplar and white oak soils. Again, with decreasing particle size of MAOM the contribution of fungi increased, demonstrating a larger contribution of ECM fungi (22–43%) together with SAP fungi (23–42%) to the small MAOM fraction. The contribution of AM fungi was only relevant for the small MAOM fraction (5–11%).

Fungal-derived C contributed 42.7% ± 6 to the C in MAOM and 28.9% ± 3 in POM fractions and was generally independent from tree species (Supporting material Fig. S5, except for significantly less fungal C in MAOM under white oak ($t = 6.422$, df = 4, $P = 0.003$). Hence, the

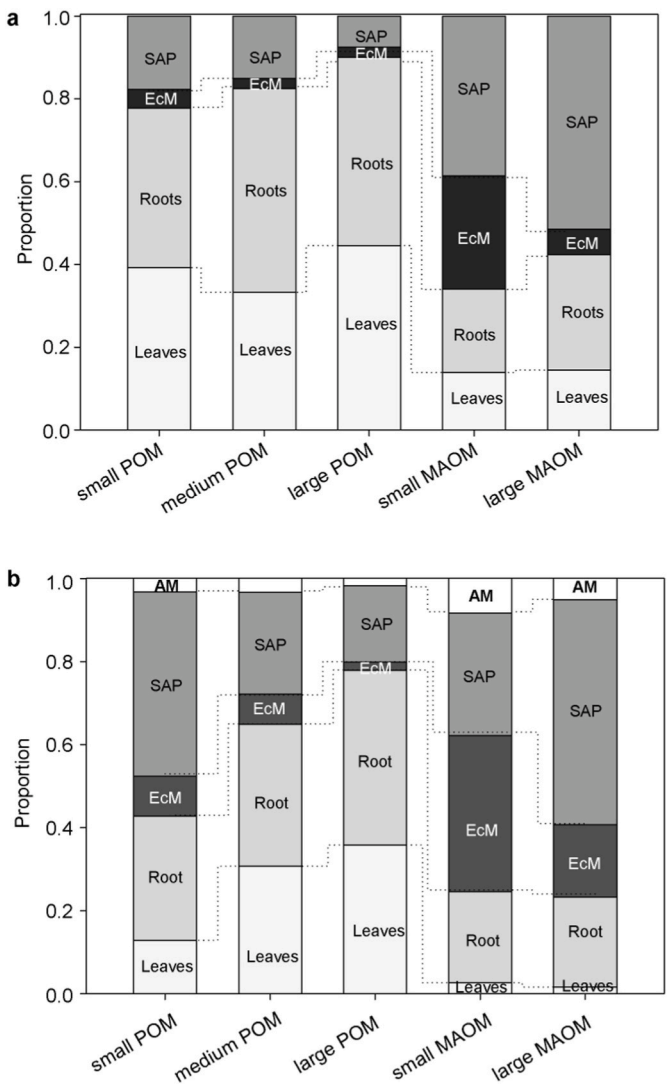

Fig. 2. Stacked bar plot of input contributions to various POM and MAOM fractions under white oak (a) and tulip poplar (b). Inputs were separated into leaves (light grey), roots (grey) ectomycorrhizal fungi (ECM, dark grey), saprotrophic fungi (SAP, medium grey) and arbuscular mycorrhizal fungi (AM, white).

portion of fungal-derived C was almost doubled in MAOM as compared to POM fractions. In contrast, bacterial-derived C contributed 12.1% ± 2 to MAOM-C and 2.1% ± 1 to POM-C fractions.

Total amino sugars, fungal residue correlated glucosamine and bacterial residue related muramic acid indicated that both the POM and MAOM fractions were comprised of more fungal relative to bacterial residues ($U(8,8) = 36$, $P < 0.001$; Fig. 3, Supporting material Fig. S5). The portion of fungal C was highest for POM under white oak (Fig. 3, $t = -3.46$, $df = 6$, $P = 0.014$). However, the portions of fungal C in total C was elevated in MAOM fractions by about 40% (Fig. 3) due to the low total C contents in MAOM (Supporting material Table S1).

4. Discussion

Our study used stable isotope analyses in a Bayesian Inference mixing model accompanied by amino sugar analyses to determine the contribution of plant and microbial C and N to various SOM fractions. While we found that plant-related inputs dominated POM fractions, a shift to fungal-related inputs occurred for MAOM fractions, with SAP fungi dominating over ECM fungi regardless of the associated tree. Of

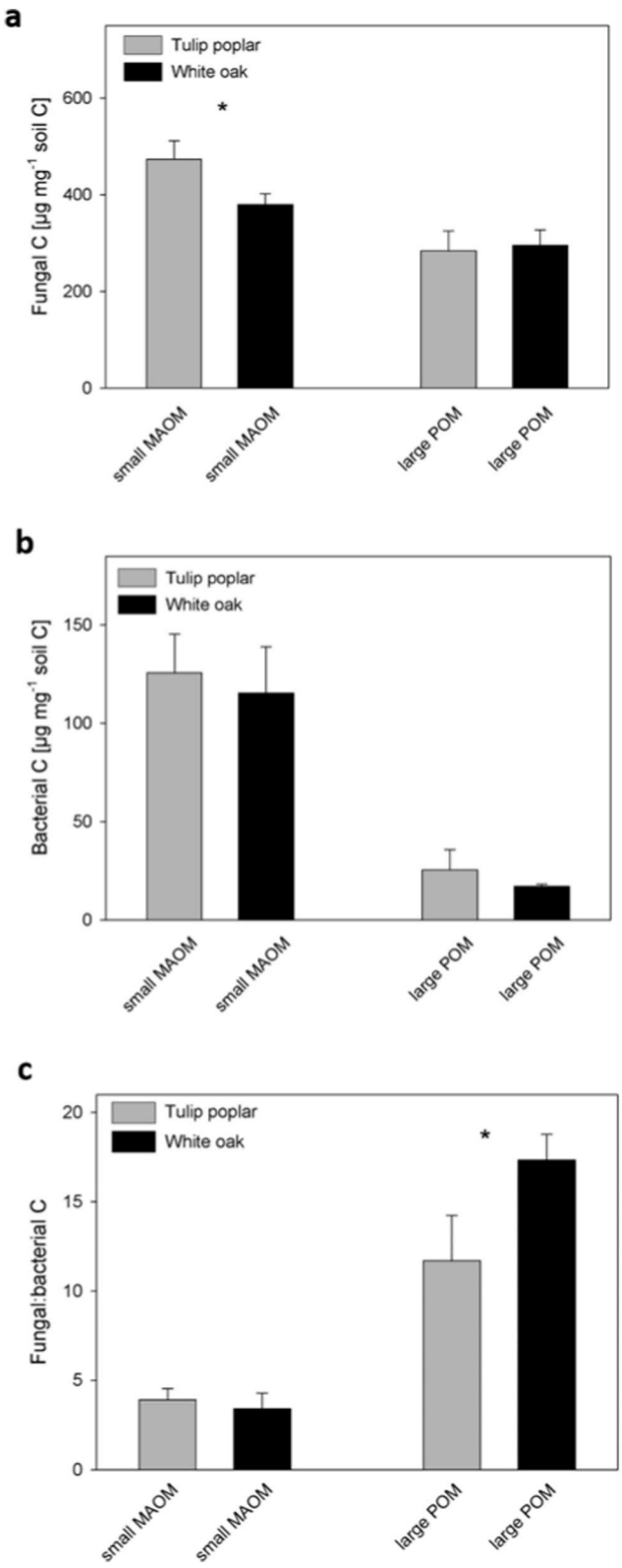

Fig. 3. Bar plots (with SD) of amounts of fungal and bacterial residue C and fungal to bacterial residue C ratio in small (<20 µm) MAOM and large (>63 µm) POM fractions based on amino sugar data. (a) Fungal C in µg per mg soil C for small MAOM and large POM fractions of tulip poplar and white oak. (b) Bacterial C in µg per mg soil for small MAOM and large POM fractions of tulip poplar and white oak. (c) Ratio of fungal to bacterial C in the small MAOM and large POM fractions of tulip poplar and white oak. Significant differences ($P < 0.05$) between tree species are indicated by an asterisk (*).

the microbial residues, fungal C predominantly contributes to POM fractions, whereas fungal and bacterial C were both important contributors to MAOM fractions. These differences in microbial contributions imply different microbial groups affecting C and N storage in POM *vs*. MAOM fractions.

4.1. Stable isotope patterns

In general, the $\delta^{13}C$, $\delta^{15}N$ isotopic composition of the MAOM fractions shifted towards the isotopic values of fungi, particularly ECM fungi in our study. We argue that this results from the predominant contribution of fungal biomass (necromass) to these fractions. The $\delta^{13}C$ and $\delta^{15}N$ isotope signature of fungi is typically a function of their C and N sources, metabolic (including degradative capabilities) and fractionation processes (e.g. Gleixner et al., 1993; Taylor et al., 1997; Kohzu et al., 1999; Hobbie et al., 2012), leading to an enrichment relative to plant tissues.

Historically, it was believed that decomposition occurred via preferential decay of easily accessible compounds depleted in ^{13}C (discussed in Ehleringer et al., 2000; Menichetti et al., 2015), leaving behind ^{13}C enriched compounds and potentially interfering with the use of isotopic mixing models to determine the source of SOM. For instance, Menichetti et al. (2015) described a ^{13}C enrichment of ~2‰ of bulk soil over the duration of SOM decay at long-term bare fallow sites with arrested C inputs, aligning with the ^{13}C enrichment from POM to MAOM fractions in our study. Preferential decay of depleted C compounds (e.g. lignin, lipids) was considered to explain the increase in ^{13}C in older SOM compartments over time, also leading to an increase in ^{13}C of SOM with soil depth (Nadelhoffer and Fry, 1988; Kohl et al., 2015). Yet, this assumption is not entirely consistent with the observed ^{13}C-depletion of some plant residues in soil with longer residence times. Lignin, for instance, is ^{13}C depleted, whereas rapidly utilized primary sugars are ^{13}C enriched (Gleixner et al., 1993). Thus, lignin accumulation in deeper soil layers should favor a ^{13}C depletion rather than an ^{13}C enrichment. However, selective preservation of ^{13}C-depleted litter components *per se* has long been questioned in the literature (Marschner et al., 2008; Nadelhoffer and Fry, 1988). Rather, it has been argued that ^{13}C enrichment in older parts of the soil, e.g., along the depth profile, is due to a higher contribution of microbial residues. As a result of carboxylation reactions, microbes are enriched in ^{13}C relative to their food source (Ehleringer et al., 2000). This is also consistent with a study by Kohl et al. (2015) showing that ^{13}C enrichment along a depth profile is attributable to a shift in fungal and bacterial biomass proportions, rather than ^{13}C-enrichment caused by preferential decomposition of ^{12}C. Therefore, we argue that an accumulation of ^{13}C enriched microbial residues is the most reliable explanation for the similarity of our MAOM fractions and fungal biomass, allowing for the application and interpretation of the endmember mixing model.

Plant-related and fungal-related C and N isotopic signatures embed POM and MAOM fractions' isotopic signatures, indicating a shift in isotopic enrichment from plant to microbial tissue inputs to SOM fractions and suggesting a preferential preservation of ^{13}C enriched microbial biomass deposits in a temperate deciduous forest. The high contribution of fungal inputs particularly to MAOM in our study conforms with mechanistic microbial model estimates of the contribution of microbial-derived C to SOM ranging from 47% to 80% depending on environment-specific factors such as litter input rate, biomass and necromass turnover or fungal to bacterial ratios (Fan and Liang, 2015; Liang et al., 2019). However, other studies showed a contribution of microbial C to stable SOM smaller than 50%, while plant-related inputs were more important (Angst et al., 2021). While also our MAOM fractions contained plant-related soil C, the dominance of microbially-related soil C with ~60% was evident.

The transfer of the Bayesian Inference isotopic mixing model frequently applied in food web studies to the soil system performed in our study represents a first estimate of the applicability of this method for the soil system and may serve as a basis for future research. The results of a major fungal contribution to MAOM fractions were supported by the amino sugar data. The inbuilt mixing model algorithm did not show any problems with the raw data input and the result output. In future fractionation factors may enhance the model output; whereby currently the precise fractionations factors are as yet mostly undefined in our system.

4.2. Amino sugar patterns

Our results provide insights into the fate of plant- and microbial-derived OM in POM and MAOM fractions. The high contribution of fungal residues to POM fractions and the contribution of both fungal and bacterial residues to MAOM fractions as based on amino sugar analyses demonstrate the dominant role of microbes for soil C and N stabilization in mineral associations. These estimates fit with results by Vidal et al. (2021) demonstrating that hyphae of saprotrophic fungi transfer C and N from needle litter to surrounding bulk soil where fungal residues accumulate at minerals and form MAOM. Thus, the presence and processive activity of fungi in plant-dominated POM fractions represents a necessary prerequisite for the establishment of MAOM, but also acts as a transfer mechanism of C and N from POM and MAOM fractions (cf. Vidal et al., 2021).

While we were not able to include bacteria in isotopic analyses and, hence, to our mixing model, their isotopic signatures likely would have shown an even stronger ^{13}C enrichment relative to SAP fungi as reported by Kohl et al. (2015) from PLFA analyses. Hence, we would expect a smaller contribution of bacterial residues to MAOM fractions compared to fungal residues as also indicated by the amino sugar data. Future analysis of the C and N isotopic signature of amino sugars may aid to elucidate the influence of bacterial and fungal residues on SOM fractions more closely. This might be combined with compound-specific analysis to trace the fate of different compounds from various sources to POM and MAOM fractions. Additionally, PLFA-SIP and AS-SIP analysis may provide more detailed information on microbe contributions in future studies.

4.3. Role of mycorrhizal association for SOM

Despite an expected difference between ECM (oak) and AM (tulip poplar) systems in nutrient cycling and litter quality (e.g. Phillips et al., 2013; Midgley et al., 2015), we found few notable isotopic differences between fungal guilds and no tree species specific differences between tulip poplar and white oak soils. We expected ECM fungi to be the dominant contributor to MAOM for white oak and SAP fungi to be the dominant contributor to MAOM for tulip poplar. In contrast, SAP fungi were the dominant contributor to MAOM fractions for both tree species. Our analysis showed that in mixed forests the co-existence and mixing of mycorrhizal types across the soil landscape is important for soil C storage patterns. In particular, the extensive growth of mycelia (e.g. Anderson and Cairney, 2007 and literature therein) can span large soil areas and contribute to soil C and N cycling patterns. The negligible AM fungi contribution to soil fractions' C and N likely results from their low biomass production (cf. Cheeke et al., 2021), but components other than hyphae, for example, exudates such as glomalin, hydrophobins, chaplins or SC15 (Rillig, 2004; Etcheverría et al., 2009; Rillig et al., 2007) may contribute more substantially to stable SOM.

Differences between ECM- and AM-associated systems are frequently driven by the C utilization and N acquisition strategies of associated fungi (Phillips et al., 2013). A study by Keller et al. (2020) identified roots inputs as the predominant source of MAOM, with greater root C inputs in AM compared to ECM soils. This mycorrhizal type difference could result from higher exudation and faster turnover of AM root and fungal biomass (Keller et al., 2020) causing a stimulation of SAP fungal growth (Verbruggen et al., 2017). Recent literature describes the activation and fueling of saprotrophic organisms with C by AM fungi in

order to access nutrients released by enhanced SOM decomposition (Verbruggen et al., 2017; Kaiser et al., 2015). This may explain the high contribution of SAP fungal residues to the SOM fractions in the AM-associated tulip poplar system. Studies from Beidler et al. (2020) and Eagar et al. (2021) conducted in the same forest as this study further supports the expectation of AM systems being driven by saprotrophic organisms, as the authors described more saprotrophic fungi and molds in soils under AM vegetation compared to ECM vegetation. Similar findings were reported by Bahram et al. (2020) for topsoil microbiomes of sites in the Baltic region. Overall, the interaction between mycorrhizal and saprotrophic fungi appears relevant for the C and N inputs contributing to MAOM fractions.

While for AM-associated trees the facilitation of saprotrophic organisms to mine for nutrients explains the dominance of SAP fungi, for ECM-associated trees both ECM and SAP fungi are actively contributing to SOM formation.

5. Conclusion

Our study provides clear evidence for the high contribution of fungal biomass for the build-up of MAOM. This clearly highlights the importance of both, mycorrhizal and saprotrophic fungi, for the formation of persistent SOM. Thus, our results underpin the need to consider fungal contributions to SOM for predictions of soil C and N storage and release.

Author contributions

SK, RPP and JP developed the research design. SK and AK conducted the field survey and performed the laboratory analyses accompanied by AJW, VLB and NM. SK and NM analyzed the results. SK wrote the first draft of the manuscript. All coauthors contributed to the manuscript.

Data statement

The raw data are available in the Supporting material (Supporting material Table S3).

Declaration of competing interest

The authors declare that they have no known competing financial interests or personal relationships that could have appeared to influence the work reported in this paper.

Acknowledgements

We want to thank IU RTP and preserve manager Michael Chitwood. Special thanks to Elizabeth Huenupi-Pena for assistance with organizing field and lab equipment and shipping and to Ilse Thaufelder for helping with sampling and sample preparation. We thank Steven Russell and Ronald Kerner for their help with fungal sporocarp identification. Thanks to Sofia Gomes for DNA analyses of fungi in tree roots. Many thanks to the BayCEER Laboratory of Isotope Biogeochemistry (University of Bayreuth, Germany) and the Centre for Stable Isotope Research and Analysis (Georg-August-University Göttingen, Germany) for stable isotope analyses. This work was funded by the German Research Foundation (DFG) under project PA 2377/2-1/GU 1309/5-1 “Towards a predictive understanding on how mycorrhizal types influence the decomposition of soil organic matter”. Part of the lab work and chemical analyzes were funded by the DFG project “Rhizosphere as driver of subsoil organic matter distribution and composition” (MU3021/4-2) in the frame of the research unit “The Forgotten Part of Carbon Cycling: Soil Organic Matter Storage and Turnover in Subsoils (SUBSOM)” (FOR1806).

Appendix A. Supplementary data

Supplementary data to this article can be found online at https://doi.org/10.1016/j.soilbio.2022.108634.

References

Amelung, W., 2001. Methods using amino sugars as markers for microbial residues in soil. Assessment Methods for Soil Carbon 233–270.
Amelung, W., Zech, W., 1999. Minimisation of organic matter disruption during particle-size fractionation of grassland epipedons. Geoderma 92, 73–85.
Anderson, I.C., Cairney, J.W.G., 2007. Ectomycorrhizal fungi: exploring the mycelial frontier. FEMS Microbiology Reviews 31, 388–406.
Angst, G., Mueller, K.E., Kögel-Knabner, I., Freeman, K.H., Mueller, C.W., 2017. Aggregation controls the stability of lignin and lipids in clay-sized particulate and mineral associated organic matter. Biogeochemistry 132, 307–324.
Angst, G., Mueller, K.E., Nierop, K.G.J., Simpson, M.J., 2021. Plant- or microbial-derived? A review on the molecular composition of stabilized soil organic matter. Soil Biology and Biochemistry 156, 108189.
Appuhn, A., Joergensen, R.G., 2006. Microbial colonisation of roots as a function of plant species. Soil Biology and Biochemistry 38, 1040–1051.
Bahram, M., Netherway, T., Hildebrand, F., Pritsch, K., Drenkhan, R., Loit, K., Anslan, S., Bork, P., Tedersoo, L., 2020. Plant nutrient-acquisition strategies drive topsoil microbiome structure and function. New Phytologist 227, 1189–1199.
Baldock, J.A., Skjemstad, J.O., 2000. Role of the soil matrix and minerals in protecting natural organic materials against biological attack. Organic Geochemistry 31, 697–710.
Beidler, K.V., Phillips, R.P., Andrews, E., Maillard, F., Mushinski, R.M., Kennedy, P.G., 2020. Substrate quality drives fungal necromass decay and decomposer community structure under contrasting vegetation types. Journal of Ecology 108, 1845–1859.
Bond, A.L., Diamond, A.W., 2011. Recent Bayesian stable-isotope mixing models are highly sensitive to variation in discrimination factors. In: Ecological Applications, vol. 21. a publication of the Ecological Society of America, pp. 1017–1023.
Bradford, M.A., Keiser, A.D., Davies, C.A., Mersmann, C.A., Strickland, M.S., 2013. Empirical evidence that soil carbon formation from plant inputs is positively related to microbial growth. Biogeochemistry 113, 271–281.
Castellano, M.J., Mueller, K.E., Olk, D.C., Sawyer, J.E., Six, J., 2015. Integrating plant litter quality, soil organic matter stabilization, and the carbon saturation concept. Global Change Biology 21, 3200–3209.
Cheeke, T.E., Phillips, R.P., Kuhn, A., Rosling, A., Fransson, P., 2021. Variation in hyphal production rather than turnover regulates standing fungal biomass in temperate hardwood forests. Ecology 102, e03260.
Christensen, B.T., 2001. Physical fractionation of soil and structural and functional complexity in organic matter turnover. European Journal of Soil Science 52, 345–353.
Córdova, S.C., Olk, D.C., Dietzel, R.N., Mueller, K.E., Archontouilis, S.V., Castellano, M. J., 2018. Plant litter quality affects the accumulation rate, composition, and stability of mineral-associated soil organic matter. Soil Biology and Biochemistry 125, 115–124.
Cotrufo, M.F., Ranalli, M.G., Haddix, M.L., Six, J., Lugato, E., 2019. Soil carbon storage informed by particulate and mineral-associated organic matter. Nature Geoscience 12, 989–994.
Cotrufo, M.F., Wallenstein, M.D., Boot, C.M., Denef, K., Paul, E., 2013. The Microbial Efficiency-Matrix Stabilization (MEMS) framework integrates plant litter decomposition with soil organic matter stabilization: do labile plant inputs form stable soil organic matter? Global Change Biology 19, 988–995.
Craig, M.E., Turner, B.L., Liang, C., Clay, K., Johnson, D.J., Phillips, R.P., 2018. Tree mycorrhizal type predicts within-site variability in the storage and distribution of soil organic matter. Global Change Biology 24, 3317–3330.
Cyle, K.T., Hill, N., Young, K., Jenkins, T., Hancock, D., Schroeder, P.A., Thompson, A., 2016. Substrate quality influences organic matter accumulation in the soil silt and clay fraction. Soil Biology and Biochemistry 103, 138–148.
Eagar, A.C., Mushinski, R.M., Horning, A.L., Smemo, K.A., Phillips, R.P., Blackwood, C. B., 2021. Arbuscular mycorrhizal tree communities have greater soil fungal diversity and relative abundances of saprotrophs and pathogens compared to ectomycorrhizal tree communities. Applied and Environmental Microbiology AEM0178221.
Ehleringer, J.R., Buchmann, N., Flanagan, L.B., 2000. Carbon isotope ratios in belowground carbon cycle processes. In: Ecological Applications, vol. 10. a publication of the Ecological Society of America, pp. 412–422.
Etcheverría, P., Huygens, D., Godoy, R., Borie, F., Boeckx, P., 2009. Arbuscular mycorrhizal fungi contribute to 13C and 15N enrichment of soil organic matter in forest soils. Soil Biology and Biochemistry 41, 858–861.
Evans, L.R., Pierson, D., Lajtha, K., 2020. Dissolved organic carbon production and flux under long-term litter manipulations in a Pacific Northwest old-growth forest. Biogeochemistry 149, 75–86.
Fan, Z., Liang, C., 2015. Significance of microbial asynchronous anabolism to soil carbon dynamics driven by litter inputs. Scientific Reports 5, 9575.
Faust, S., Heinze, S., Ngosong, C., Sradnick, A., Oltmanns, M., Raupp, J., Geisseler, D., Joergensen, R.G., 2017. Effect of biodynamic soil amendments on microbial communities in comparison with inorganic fertilization. Applied Soil Ecology 114, 82–89.
Fernandez, Christopher W., Kennedy, Peter G., 2016. Revisiting the ‘Gadgil effect’: do interguild fungal interactions control carbon cycling in forest soils? New Phytologist 209, 1382–1394. https://doi.org/10.1111/nph.13648.

Frey, S.D., 2019. Mycorrhizal fungi as mediators of soil organic matter dynamics. Annual Review of Ecology, Evolution and Systematics 50, 237–259.
Fry, B., 2008. Stable Isotope Ecology. Springer, New York.
Gebauer, G., Dietrich, P., 1993. Nitrogen isotope ratios in different compartments of a mixed stand of spruce, larch and beech trees and of understorey vegetation including fungi. Isotopenpraxis Isotopes in Environmental and Health Studies 29, 35–44.
Gebauer, G., Taylor, A.F.S., 1999. ^{15}N natural abundance in fruit bodies of different functional groups of fungi in relation to substrate utilization. New Phytologist 142, 93–101.
Gleixner, G., Danier, H.J., Werner, R.A., Schmidt, H.L., 1993. Correlations between the 13C content of primary and secondary plant products in different cell compartments and that in decomposing basidiomycetes. Plant Physiology 102, 1287–1290.
Godbold, D.L., Hoosbeek, M.R., Lukac, M., Cotrufo, M.F., Janssens, I.A., Ceulemans, R., Polle, A., Velthorst, E.J., Scarascia-Mugnozza, G., Angelis, P. de, Miglietta, F., Peressotti, A., 2006. Mycorrhizal hyphal turnover as a dominant process for carbon input into soil organic matter. Plant and Soil 281, 15–24.
Golchin, A., Oades, J.M., Skjemstad, J.O., Clarke, P., 1994. Soil structure and carbon cycling. Soil Research 32, 1043.
Guerrant, G.O., Moss, C.W., 1984. Determination of monosaccharides as aldononitrile, O-methyloxime, alditol, and cyclitol acetate derivatives by gas chromatography. Analytical Chemistry 56, 633–638.
Hobbie, E.A., Sánchez, F.S., Rygiewicz, P.T., 2012. Controls of isotopic patterns in saprotrophic and ectomycorrhizal fungi. Soil Biology and Biochemistry 48, 60–68.
Högberg, M.N., Högberg, P., 2002. Extramatrical ectomycorrhizal mycelium contributes one-third of microbial biomass and produces, together with associated roots, half the dissolved organic carbon in a forest soil. New Phytologist 154, 791–795.
Högberg, P., Plamboeck, A.H., Taylor, A.F., Fransson, P.M., 1999. Natural (13)C abundance reveals trophic status of fungi and host-origin of carbon in mycorrhizal fungi in mixed forests. In: Proceedings of the National Academy of Sciences of the United States of America, vol. 96, pp. 8534–8539.
Huang, W., Hammel, K.E., Hao, J., Thompson, A., Timokhin, V.I., Hall, S.J., 2019. Enrichment of lignin-derived carbon in mineral-associated soil organic matter. Environmental Science and Technology 53, 7522–7531.
Joergensen, R.G., 2018. Amino sugars as specific indices for fungal and bacterial residues in soil. Biology and Fertility of Soils 54, 559–568.
Kaiser, C., Kilburn, M.R., Clode, P.L., Fuchslueger, L., Koranda, M., Cliff, J.B., Solaiman, Z.M., Murphy, D.V., 2015. Exploring the transfer of recent plant photosynthates to soil microbes: mycorrhizal pathway vs direct root exudation. New Phytologist 205, 1537–1551.
Keller, A.B., Brzostek, E.R., Craig, M.E., Fisher, J.B., Phillips, R.P., 2020. Root-derived inputs are major contributors to soil carbon in temperate forests, but vary by mycorrhizal type. Ecology Letters 24, 626–635.
Klink, S., Giesemann, P., Hubmann, T., Pausch, J., 2020. Stable C and N isotope natural abundances of intraradical hyphae of arbuscular mycorrhizal fungi. Mycorrhiza 30, 773–780.
Kohl, L., Laganière, J., Edwards, K.A., Billings, S.A., Morrill, P.L., van Biesen, G., Ziegler, S.E., 2015. Distinct fungal and bacterial δ13C signatures as potential drivers of increasing δ13C of soil organic matter with depth. Biogeochemistry 124, 13–26.
Kohzu, A., Yoshioka, T., Ando, T., Takahashi, M., Koba, K., Wada, E., 1999. Natural 13 C and 15 N abundance of field-collected fungi and their ecological implications. New Phytologist 144, 323–330.
Kopittke, P.M., Dalal, R.C., Hoeschen, C., Li, C., Menzies, N.W., Mueller, C.W., 2020. Soil organic matter is stabilized by organo-mineral associations through two key processes: the role of the carbon to nitrogen ratio. Geoderma 357, 113974.
Kopittke, P.M., Hernandez-Soriano, M.C., Dalal, R.C., Finn, D., Menzies, N.W., Hoeschen, C., Mueller, C.W., 2018. Nitrogen-rich microbial products provide new organo-mineral associations for the stabilization of soil organic matter. Global Change Biology 24, 1762–1770.
Lavallee, J.M., Soong, J.L., Cotrufo, M.F., 2020. Conceptualizing soil organic matter into particulate and mineral-associated forms to address global change in the 21st century. Global Change Biology 26, 261–273.
Lehmann, J., Hansel, C.M., Kaiser, C., Kleber, M., Maher, K., Manzoni, S., Nunan, N., Reichstein, M., Schimel, J.P., Torn, M.S., Wieder, W.R., Kögel-Knabner, I., 2020. Persistence of soil organic carbon caused by functional complexity. Nature Geoscience 13, 529–534.
Lehmann, J., Kleber, M., 2015. The contentious nature of soil organic matter. Nature 528, 60–68.
Li, N., Xu, Y.-Z., Han, X.-Z., He, H.-B., Zhang, X.-d., Zhang, B., 2015. Fungi contribute more than bacteria to soil organic matter through necromass accumulation under different agricultural practices during the early pedogenesis of a Mollisol. European Journal of Soil Biology 67, 51–58.
Liang, C., Amelung, W., Lehmann, J., Kästner, M., 2019. Quantitative assessment of microbial necromass contribution to soil organic matter. Global Change Biology 25, 3578–3590.
Lützow, M. von, Kögel-Knabner, I., Ekschmitt, K., Flessa, H., Guggenberger, G., Matzner, E., Marschner, B., 2007. SOM fractionation methods: relevance to functional pools and to stabilization mechanisms. Soil Biology and Biochemistry 39, 2183–2207.
Marschner, B., Brodowski, S., Dreves, A., Gleixner, G., Gude, A., Grootes, P.M., Hamer, U., Heim, A., Jandl, G., Ji, R., Kaiser, K., Kalbitz, K., Kramer, C., Leinweber, P., Rethemeyer, J., Schäffer, A., Schmidt, M.W.I., Schwark, L., Wiesenberg, G.L.B., 2008. How relevant is recalcitrance for the stabilization of organic matter in soils? Journal of Plant Nutrition and Soil Science 171, 91–110.
Menichetti, L., Houot, S., van Oort, F., Kätterer, T., Christensen, B.T., Chenu, C., Barré, P., Vasilyeva, N.A., Ekblad, A., 2015. Increase in soil stable carbon isotope ratio relates to loss of organic carbon: results from five long-term bare fallow experiments. Oecologia 177, 811–821.
Midgley, M.G., Brzostek, E., Phillips, R.P., 2015. Decay rates of leaf litters from arbuscular mycorrhizal trees are more sensitive to soil effects than litters from ectomycorrhizal trees. Journal of Ecology 103, 1454–1463.
Midgley, M.G., Phillips, R.P., 2016. Resource stoichiometry and the biogeochemical consequences of nitrogen deposition in a mixed deciduous forest. Ecology 97, 3369–3378.
Midgley, M.G., Phillips, R.P., 2019. Spatio-temporal heterogeneity in extracellular enzyme activities tracks variation in saprotrophic fungal biomass in a temperate hardwood forest. Soil Biology and Biochemistry 138, 107600.
Mikutta, R., Turner, S., Schippers, A., Gentsch, N., Meyer-Stüve, S., Condron, L.M., Peltzer, D.A., Richardson, S.J., Eger, A., Hempel, G., Kaiser, K., Klotzbücher, T., Guggenberger, G., 2019. Microbial and abiotic controls on mineral-associated organic matter in soil profiles along an ecosystem gradient. Scientific Reports 9, 10294.
Mueller, C.W., Gutsch, M., Kothieringer, K., Leifeld, J., Rethemeyer, J., Brueggemann, N., Kögel-Knabner, I., 2014. Bioavailability and isotopic composition of CO2 released from incubated soil organic matter fractions. Soil Biology and Biochemistry 69, 168–178.
Mueller, C.W., Koegel-Knabner, I., 2009. Soil organic carbon stocks, distribution, and composition affected by historic land use changes on adjacent sites. Biology and Fertility of Soils 45, 347–359.
Mushinski, R.M., Payne, Z.C., Raff, J.D., Craig, M.E., Pusede, S.E., Rusch, D.B., White, J. R., Phillips, R.P., 2020. Nitrogen cycling microbiomes are structured by plant mycorrhizal associations with consequences for nitrogen oxide fluxes in forests. Global Change Biology 27, 1068–1082.
Mushinski, R.M., Phillips, R.P., Payne, Z.C., Abney, R.B., Jo, I., Fei, S., Pusede, S.E., White, J.R., Rusch, D.B., Raff, J.D., 2019. Microbial mechanisms and ecosystem flux estimation for aerobic NOy emissions from deciduous forest soils. In: Proceedings of the National Academy of Sciences of the United States of America, vol. 116, pp. 2138–2145.
Nadelhoffer, K.J., Fry, B., 1988. Controls on natural nitrogen-15 and carbon-13 abundances in forest soil organic matter. Soil Science Society of America Journal 52, 1633–1640.
Parnell, A., Jackson, A., 2013. Siar: Stable Isotope Analysis in R.
Parnell, A.C., Inger, R., Bearhop, S., Jackson, A.L., 2010. Source partitioning using stable isotopes: coping with too much variation. PLoS One 5, e9672.
Parsons, J.W., 1981. Chemistry and distribution of amino sugars in soils and soil organisms. Soil Biochemistry 5, 197–227.
Phillips, R.P., Brzostek, E., Midgley, M.G., 2013. The mycorrhizal-associated nutrient economy: a new framework for predicting carbon-nutrient couplings in temperate forests. New Phytologist 199, 41–51.
Poeplau, C., Don, A., Six, J., Kaiser, M., Benbi, D., Chenu, C., Cotrufo, M.F., Derrien, D., Gioacchini, P., Grand, S., Gregorich, E., Griepentrog, M., Gunina, A., Haddix, M., Kuzyakov, Y., Kühnel, A., Macdonald, L.M., Soong, J., Trigalet, S., Vermeire, M.-L., Rovira, P., van Wesemael, B., Wiesmeier, M., Yeasmin, S., Yevdokimov, I., Nieder, R., 2018. Isolating organic carbon fractions with varying turnover rates in temperate agricultural soils – a comprehensive method comparison. Soil Biology and Biochemistry 125, 10–26.
Rillig, M.C., 2004. Arbuscular mycorrhizae, glomalin, and soil aggregation. Canadian Journal of Soil Science 84, 355–363.
Rillig, M.C., Caldwell, B.A., Wösten, H.A.B., Sollins, P., 2007. Role of proteins in soil carbon and nitrogen storage: controls on persistence. Biogeochemistry 85, 25–44.
Rosling, A., Midgley, M.G., Cheeke, T., Urbina, H., Fransson, P., Phillips, R.P., 2016. Phosphorus cycling in deciduous forest soil differs between stands dominated by ecto- and arbuscular mycorrhizal trees. New Phytologist 209, 1184–1195.
Rumpel, C., Baumann, K., Remusat, L., Dignac, M.-F., Barré, P., Deldicque, D., Glasser, G., Lieberwirth, I., Chabbi, A., 2015. Nanoscale evidence of contrasted processes for root-derived organic matter stabilization by mineral interactions depending on soil depth. Soil Biology and Biochemistry 85, 82–88.
Schmidt, M.W.I., Rumpel, C., Kögel-Knabner, I., 1999. Evaluation of an ultrasonic dispersion procedure to isolate primary organomineral complexes from soils. European Journal of Soil Science 50, 87–94.
Schmidt, M.W.I., Torn, M.S., Abiven, S., Dittmar, T., Guggenberger, G., Janssens, I.A., Kleber, M., Kögel-Knabner, I., Lehmann, J., Manning, D.A.C., Nannipieri, P., Rasse, D.P., Weiner, S., Trumbore, S.E., 2011. Persistence of soil organic matter as an ecosystem property. Nature 478, 49–56.
Schöning, I., Morgenroth, G., Kögel-Knabner, I., 2005. O/N-alkyl and alkyl C are stabilised in fine particle size fractions of forest soils. Biogeochemistry 73, 475–497.
Sigma, 2008. Plot Version 11.0. Systat Software, San Jose, USA.
Software R version 3.6.1, 2019. R: A Language and Environment for Statistical Computing. R Development Core Team, Vienna, Austria.
Sokol, N.W., Bradford, M.A., 2019. Microbial formation of stable soil carbon is more efficient from belowground than aboveground input. Nature Geoscience 12, 46–53.
Taylor, A.F.S., Högbom, L., Högberg, M., Lyon, A.J.E., Näsholm, T., Högberg, P., 1997. Natural 15 N abundance in fruit bodies of ectomycorrhizal fungi from boreal forests. New Phytologist 136, 713–720.
Verbruggen, E., Pena, R., Fernandez, C.W., Soong, J.L., 2017. Mycorrhizal interactions with saprotrophs and impact on soil carbon storage. In: Johnson, N. (Ed.), Mycorrhizal Mediation of Soil. Elsevier, pp. 441–460 [Place of publication not identified].
Vidal, A., Klöffel, T., Guigue, J., Angst, G., Steffens, M., Hoeschen, C., Mueller, C.W., 2021. Visualizing the transfer of organic matter from decaying plant residues to soil mineral surfaces controlled by microorganisms. Soil Biology and Biochemistry 160, 108347.

Wagai, R., Mayer, L.M., Kitayama, K., 2009. Nature of the "occluded" low-density fraction in soil organic matter studies: a critical review. Soil Science & Plant Nutrition 55, 13–25.
Witzgall, K., Vidal, A., Schubert, D.I., Höschen, C., Schweizer, S.A., Buegger, F., Pouteau, V., Chenu, C., Mueller, C.W., 2021. Particulate organic matter as a functional soil component for persistent soil organic carbon. Nature Communications 12, 4115.
Zhang, X., Amelung, W., 1996. Gas chromatographic determination of muramic acid, glucosamine, mannosamine, and galactosamine in soils. Soil Biology and Biochemistry 28, 1201–1206.